

$s + is$ State with Broken Time Reversal Symmetry in Fe-Based Superconductors

Saurabh Maiti, Andrey V. Chubukov

Department of Physics, University of Wisconsin, Madison, Wisconsin 53706, USA

(Dated: October 18, 2018)

We analyze the evolution of the superconducting gap structure in strongly hole doped $\text{Ba}_{1-x}\text{K}_x\text{Fe}_2\text{As}_2$ between $x = 1$ and $x \sim 0.4$ (optimal doping). In the latter case, the pairing state is most likely $s\pm$, with different gap signs on hole and electron pockets, but with the same signs of the gap on the two Γ -centered hole pockets (a $++$ state on hole pockets). In a pure KFe_2As_2 ($x = 1$), which has only hole pockets, laser ARPES data suggested another $s\pm$ state, in which the gap changes sign between hole pockets (a $+-$ state). We analyze how $++$ gap transforms into a $+-$ gap as $x \rightarrow 1$. We found that this transformation occurs via an intermediate $s + is$ state in which the gaps on the two hole pockets differ in phase by ϕ , which gradually involves from $\phi = \pi$ (the $+-$ state) to $\phi = 0$ (the $++$ state). This state breaks time-reversal symmetry and has huge potential for applications. We compute the dispersion of collective excitations and show that two different Leggett-type phase modes soften at the two end points of TRSB state.

I. INTRODUCTION

The high interest in iron based superconductors (FeSC) is primarily due to two key reasons. The first is a hope that the analysis of FeSCs will not only resolve the pairing mechanism in these systems but also provide important insights into the electronic pairing in a generic high- T_c superconductor. The second is a hope to explore multi-band structure of FeSCs and discover novel exotic superconducting states which have not been observed in other systems. Out of such novel superconducting states, the most searched for are the ones which break time-reversal symmetry. A spin-triplet time-reversal symmetry broken (TRSB) $p_x \pm ip_y$ state has likely been found in Sr_2RuO_4 ¹; the spin-singlet $d + id$ TRSB state has not yet been observed experimentally, although it was once proposed as a candidate state for high T_c cuprate superconductors², and was recently predicted theoretically to occur for fermions on hexagonal and honeycomb lattices near van-Hove doping³.

Several groups already searched for TRSB state in FeSCs by exploring the idea that at least in some FeSCs both s -wave and d -wave channels are attractive^{4-10,12-14}, and that one can, in principle, transform from s -wave to d -wave pairing by varying system parameters – electron¹² or hole⁹ doping, hybridization between electron pockets¹³, or degree of magnetic scattering¹⁴. In between, there is a co-existence regime in which both s and d order parameters are present, with relative phase $\pm \frac{\pi}{2}$, i.e., the system develops a TRSB $s \pm id$ superconductivity. The majority of proposals for $s + id$ state are for electron-doped FeSCs, but up to now a d -wave superconductivity has not been found in strongly electron-doped $\text{Ba}(\text{Fe}_{1-x}\text{Co}_x)_2\text{As}_2$ nor in KFe_2Se_2 -type systems which contain only electron pockets.

In this communication, we discuss another possible realization of TRSB state in FeSCs – a purely s -wave state with phase difference ϕ between superconducting order parameters on different Fermi pockets, which is not a multiple of π . The free energy of such a state is symmetric with respect to $\phi \rightarrow -\phi$. This Z_2 symmetry

(which corresponds to time reversal since $\phi \rightarrow -\phi$ implies $\Delta \rightarrow \Delta^*$) is broken when the system spontaneously chooses ϕ or $-\phi$. We label such a state as $s + is$. The $s + is$ state has been discussed in Refs 15–23 as a generic possibility of the superconducting order in the case when there are more than two Fermi pockets and as a surface state in a two-band superconductor²⁴. We show below that TRSB $s + is$ state with varying ϕ can be realized in strongly hole-doped $\text{Ba}_{1-x}\text{K}_x\text{Fe}_2\text{As}_2$ near $x = 1$.

We begin by listing several facts about $\text{Ba}_{1-x}\text{K}_x\text{Fe}_2\text{As}_2$. (i) Near optimal doping, $x \sim 0.4$, ARPES^{25,26}, neutron scattering²⁷, penetration depth²⁸ and thermal conductivity^{29,30} measurements give strong evidence for nodeless, near-constant $s\pm$ gap, which changes sign between hole and electron pockets. This is consistent with theoretical calculations^{5-8,11,31}. (ii) Recent measurements on $\text{Ba}_{1-x}\text{K}_x\text{Fe}_2\text{As}_2$ with $x = 1$ (Refs. 33,34) and $x = 0.93$ and $x = 0.88$ (Ref. 32) indicate that superconducting T_c most likely remains non-zero from $x = 0.4 \rightarrow 1$. (iii) For the $x = 1$ material KFe_2As_2 , ARPES measurements^{33,34} show that only hole pockets are present. According to theory, in this situation, both d -wave and s -wave pairing amplitudes are attractive^{5,9-11,35}, and which state wins depends on delicate interplay between system parameters. d -wave gap is the largest on the hole pocket, which in the unfolded Brillouin zone is centered at (π, π) (Refs.10,11), and s -wave gap is the largest on the two Γ -centered hole pockets (GCP's), and changes sign between them³⁵. The existing experiments point to either d -wave and s -wave gap symmetry: thermal conductivity^{36,37} and specific heat³⁸ data on KFe_2As_2 have been interpreted in favor of d -wave gap symmetry, while laser ARPES measurements³⁴ and other thermal conductivity data³⁹ have been interpreted as evidence for s -wave.

If the gap in KFe_2As_2 is d -wave, one should obviously expect a transition from d -wave to $s\pm$ state in $\text{Ba}_{1-x}\text{K}_x\text{Fe}_2\text{As}_2$ as x decreases from 1, and the region of an intermediate $s + id$ state at low T ⁹. In this work we consider what happens if the gap in KFe_2As_2 is s -wave. At a first glance, one might expect a gradual evolution

of the gap structure with x as the symmetry at $x = 1$ is the same as at optimal doping. On a more careful look, however, we note that at optimal doping the gaps on the two GCP's have equal signs (a ++ state), while in s -wave state of KFe_2As_2 they are of opposite signs (a +- state). The issue then is how a +- gap transforms into a ++ gap between $x = 1$ and optimal doping. We show that this transformation occurs via an intermediate $s + is$ state in which the relative phase ϕ of the superconducting order parameters on the two GCP's gradually evolves between π (the +- state) and 0 (the ++ state). The system spontaneously chooses either clock-wise or counter-clockwise evolution (i.e., positive or negative ϕ) and by this breaks time-reversal symmetry.

To illustrate the emergence of the $s + is$ state we first consider in Sec. 2 the minimal model with two identical GCP's and two electron pockets, all with the same density of states N_0 , and with the two angle-independent repulsive interactions $-U_{hh}$ between the two GCP's and U_{he} between hole and electron pockets. A three-band version of this model has been considered in Refs. 15,18-21,23). The interaction U_{hh} gives rise to +- gaps on the two GCP's, while U_{he} gives rise to an $s \pm$ state with different signs of the gaps on the two hole pockets. We model the doping dependence by varying the strength of hole-electron coupling U_{he} and analyze the system evolution with U_{he}/U_{hh} . We show that it occurs via a TRSB state. In Sec. 3 we extend the model and include intra-pocket repulsions and anisotropy between the two hole pockets. We show that the TRSB state still exists in a certain parameter range, but for non-equivalent hole pockets the region of TRSB state is separated from T_c line. We present our conclusions in Sec. 4. Technical details of our analysis are presented in Appendixes A-C. In Appendix C we also discuss plasmon mode in a clean 3D superconductor.

II. TRSB IN THE MINIMAL MODEL

The Hamiltonian of the minimal model is⁴⁰ $H = H_{kin} + H_{int}$, where $H_{kin} = \sum_{i,k,\alpha} \varepsilon_k (c_{ik\alpha}^\dagger c_{ik\alpha} - f_{ik\alpha}^\dagger f_{ik\alpha})$ and $H_{int} = \frac{1}{2} \sum_{k,\alpha,\beta} [U_{hh} b_{c_1k}^\dagger b_{c_2k} + \sum_{i,j} U_{he} b_{c_ik}^\dagger b_{f_ik} + h.c.]$ where $b_{xk} = \sum_{\sigma} x_{k\uparrow\sigma} x_{k\downarrow\sigma}$ and $x \in \{c_1, c_2, f_1, f_2\}$; and $i, j = 1, 2$ number the hole pockets (c) and electron pockets (f). We define superconducting gaps on two hole pockets as Δ_{h_1} and Δ_{h_2} and the gap on electron pockets as Δ_{e_1} and Δ_{e_2} . We neglect the angular dependence of U_{he} in which case $\Delta_{e_1} = \Delta_{e_2}$ because U_{he} for pockets e_1 and e_2 are equivalent due to C_4 symmetry of the underlying lattice. The equivalence between Δ_{e_1} and Δ_{e_2} persists even if we include intra-pocket interactions and inter-pocket interaction between the two electron pockets.

The set of linearized equations for Δ_{h_1} , Δ_{h_2} , and

$\Delta_{e_1} = \Delta_{e_2} = \Delta_e$ is obtained straightforwardly and reads

$$\begin{pmatrix} \Delta_{h_1} \\ \Delta_{h_2} \\ \Delta_e \end{pmatrix} = -L \begin{pmatrix} 0 & u_{hh} & 2u_{he} \\ u_{hh} & 0 & 2u_{he} \\ u_{he} & u_{he} & 0 \end{pmatrix} \begin{pmatrix} \Delta_{h_1} \\ \Delta_{h_2} \\ \Delta_e \end{pmatrix} \quad (1)$$

where $u_{he} = U_{he}N_0$, $u_{hh} = U_{hh}N_0$, N_0 is the density of states, $L \equiv \ln\left(\frac{2\Lambda}{T_c}\right)$, and Λ is the upper cut-off for the pairing. This set can be easily solved. For $u_{he} > u_{hh}/\sqrt{2}$, the eigenfunction with the largest eigenvalue is the ++ solution $(1, 1, -\gamma)$, where $\gamma = \frac{u_{hh}}{4u_{he}} + \sqrt{1 + \left(\frac{u_{hh}}{4u_{he}}\right)^2}$, and for $u_{he} < u_{hh}/\sqrt{2}$, is a +- solution $(1, -1, 0)$. Precisely at $u_{he} = u_{hh}/\sqrt{2}$ the two states become degenerate and $a(1, 1, -\gamma) + b(1, -1, 0)$ with arbitrary ratio of a/b becomes an eigenfunction. To see what happens immediately below T_c at this critical u_{he}/u_{hh} we expand the Free energy in powers of Δ_{h_i} and Δ_{e_i} to fourth order and obtain (see Appendix A)

$$\mathcal{F} = \mathcal{F}_0 - K_0 (|a|^2 + |b|^2) + K_1 (|a|^2 + |b|^2)^2 + K_2 |a^2 + b^2|^2 + K_3 |a|^4 \quad (2)$$

where $K_0 \propto T_c - T$, $K_{1,2} > 0$, and $0 > K_3 > -2K_2$. Minimizing with respect to a and b we immediately obtain $b = \pm ia\sqrt{1 + \frac{K_3}{2K_2}}$, i.e., the ++ and +- states co-exist with relative phase $\pm\pi/2$. As a consequence, immediately below the degeneracy point, the system selects an $s + is$ state, which breaks time reversal symmetry (a TRSB state).

Inside the TRSB state we can set Δ_e to be real and $\Delta_{h_1} = \Delta e^{i\phi/2}$, $\Delta_{h_2} = \Delta e^{-i\phi/2}$. We solved the set of three non-linear gap equations at $T = 0$ (see Appendix B) and found that TRSB state exists between $u_{he}^{min} = 0$ and $u_{he}^{max} \approx \frac{u_{hh}}{\sqrt{2}} (1 + \frac{u_{hh}}{4} \log 2)$. At the lower boundary, the TRSB state borders +- state and the relative phase reaches $\phi = \pi$, at the upper boundary the TRSB state borders ++ state and $\phi = 0$. In between,

$$\phi = \pm 2 \arccos \left[\frac{u_{hh}}{2u_{he}} e^{(2u_{he}^2 - u_{hh}^2)/(2u_{he}^2 u_{hh})} \right] \quad (3)$$

We show the evolution of the relative phase ϕ on the two hole pockets with u_{he}/u_{hh} in Fig. 2

Combining the results at T_c and at $T = 0$, we obtain the phase diagram shown in Fig. 1 (a). The TRSB state exists in the 'triangle' which begins as a point at T_c and extends to a finite interval at $T = 0$.

A. Collective modes

The existence of phase transitions at the boundaries of the TRSB state implies that there must be soft collective excitations. In a generic multi-gap superconductor there are three types of collective excitations: (i) variation of

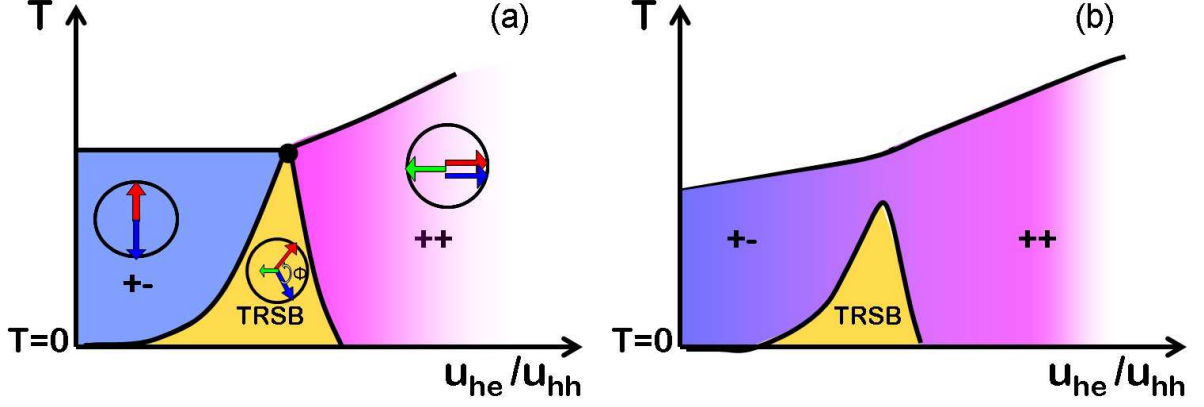


FIG. 1: Qualitative phase diagram for $\text{Ba}_{1-x}\text{K}_x\text{Fe}_2\text{As}_2$ at $x \leq 1$. We model the doping dependence by varying the ratio of inter-pocket electron-hole and hole-hole interactions u_{he}/u_{hh} which roughly scales as $1-x$. The $+-$ state has gaps of opposite signs on the two GCP's and no gap on electron pockets, the $++$ state is an ordinary $s\pm$ state in which the gaps have opposite signs on hole and electron pockets, and between them is the TRSB state. The gap structures are pictorially presented inside each region by vectors placed inside the circles. The magnitudes of the vectors represent $|\Delta_i|$ and the angles represent the phases. Cases (a) and (b) are for equal and non-equal intra-pocket interactions (u_{h1} and u_{h2}) for the two hole pockets, respectively. For (a), the TRSB state starts right at T_c and extends into a finite range at $T = 0$. For (b), the TRSB region splits off from the T_c line and is only accessible at lower temperatures, while immediately below T_c the $+-$ state gradually evolves into the $++$ state as u_{he}/u_{hh} increases.

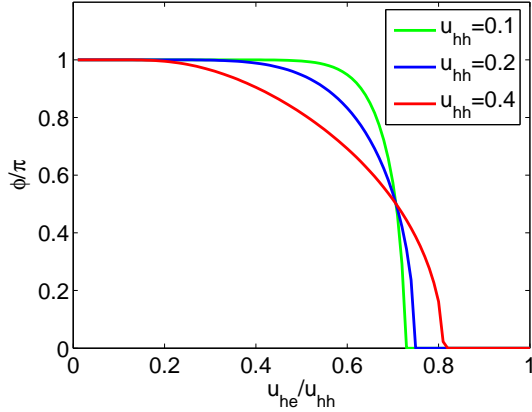


FIG. 2: Variation of the relative phase ϕ of the gaps on two hole pockets with u_{he} . This phase is zero for $u_{he} > u_{he}^{max}$, but becomes non-zero at smaller u_{he} and eventually reaches $\phi = \pm\pi$ at $u_{he} = 0$. When $|\phi|$ is between 0 and π , it can be either positive or negative, and the choice breaks Z_2 time-reversal symmetry. The width of the TRSB region is controlled by inter-pocket hole-hole interaction u_{hh} and increases when u_{hh} gets larger.

the overall phase, (ii) variations of relative phases of different gaps (Leggett modes⁴¹), and (iii) variations of the gap magnitudes. The overall phase mode is coupled by long-range Coulomb repulsion to density variations and becomes a plasmon^{42,43}. The other modes do not couple to density variations are generally either overdamped or have energy close to 2Δ . However, near the boundaries of the TRSB state, some of these modes soften.

We analyzed the dispersion of collective excitations

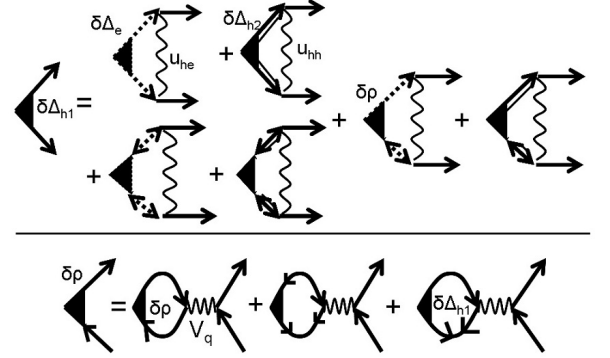


FIG. 3: The diagrammatic representation of the equations for dispersion of collective modes. The equations for other $\delta\Delta_j$ are similar to the one for $\delta\Delta_{h1}$ and are not shown. Wavy lines - interactions u_{ij} , chain-saw line - Coulomb interaction V_q . The bare vertices are not shown.

in our model by introducing small perturbations in the form of pairing and density vertices with non-zero external momentum and frequency ($\delta\Delta_{h1}, \delta\Delta_{h2}, \delta\Delta_e$, and $\delta\rho_i$, $i = 1, 2, 3$) and calculating the fully renormalized vertices (see Fig. 3). Each $\delta\Delta$ is generally a complex function $\delta\Delta_i = \delta_i^R + i\delta_i^I$, so for arbitrary momentum q , the problem reduces to solving the set of nine coupled equations for δ_i^R , δ_i^I , and $\delta\rho_i$. We verified, however, that at small q , when short-range interactions u_{hh}, u_{he} can be neglected compared to the static Coulomb interaction $V(q)$, all three $\delta\rho_i$ are equivalent, because the Coulomb repulsion does not distinguish between the different fermions (Refs. 41,44). In this approximation, i.e., $\delta\rho_i = \delta\rho$, and

the number of equations reduces to seven.

The equation for $\delta\Delta_{h_1}$ is graphically shown in Fig. 3.

Other equations are similar. In explicit form we have

$$\begin{aligned} 2\delta_i^R &= 2\delta_i^R(0) + \sum_j u_{i,j} [\Pi_{jj}^{11}\delta_j^R - \Pi_{jj}^{12}\delta_j^I + \Pi_{jj}^{13}\delta\rho_j] \\ -2\delta_i^I &= -2\delta_i^I(0) + \sum_j u_{i,j} [\Pi_{jj}^{21}\delta_j^R - \Pi_{jj}^{22}\delta_j^I + \Pi_{jj}^{23}\delta\rho_j] \\ 2\delta\rho_i &= \sum_j 2N_0V(q) [\Pi_{jj}^{31}\delta_j^R - \Pi_{jj}^{32}\delta_j^I + \Pi_{jj}^{33}\delta\rho_j] \end{aligned} \quad (4)$$

where $\delta(0)$ are bare pairing and density vertices which we introduced as small corrections to the Hamiltonian (see Appendix C), $V(q)$ is long-range Coulomb potential, and the components of the matrix u_{ij} are

$$u_{i,j} = \begin{pmatrix} 0 & u_{hh} & 2u_{he} \\ u_{hh} & 0 & 2u_{he} \\ u_{he} & u_{he} & 0 \end{pmatrix} \quad (5)$$

Further, $\Pi_{ii}^{ab} = \Pi_{ii}^{ab}(q, \Omega) = \frac{1}{N_0} \int d^2k d\omega / (2\pi)^3 \text{Tr} [\mathcal{G}_i(k, \omega) \sigma^a \mathcal{G}_i(k+q, \omega+\Omega) \sigma^b]$, where σ^a are Pauli matrices, \mathcal{G}_i are Nambu Green's function of a superconductor, $i \in \{c_1, c_2, e\}$.

In explicit form we have (see Appendix C for details)

$$\begin{aligned} \Pi_{ii}^{11}(\vec{q}, \Omega) &= - \left[2L_i - 1 - \cos\phi - \left(\frac{4}{3} - \frac{2}{3} \cos\phi \right) X_i^2 \right] \\ \Pi_{ii}^{22}(\vec{q}, \Omega) &= - \left[2L_i - 1 + \cos\phi - \left(\frac{4}{3} + \frac{2}{3} \cos\phi \right) X_i^2 \right] \\ \Pi_{ii}^{33}(\vec{q}, \Omega) &= - \left[2 - \frac{4}{3} \left(\frac{\Omega}{2\Delta_i} \right)^2 \right] \\ \Pi_{ii}^{12}(\vec{q}, \Omega) &= - \sin\phi \left[1 - \frac{2}{3} X_i^2 \right] \\ &= \Pi_{ii}^{21}(\vec{q}, \Omega) \\ \Pi_{ii}^{13}(\vec{q}, \Omega) &= - \frac{i\Omega}{\Delta_i} \sin\frac{\phi}{2} \left[1 - \frac{2}{3} X_i^2 \right] \\ &= -\Pi_{ii}^{31}(\vec{q}, \Omega) \\ \Pi_{ii}^{23}(\vec{q}, \Omega) &= - \frac{i\Omega}{\Delta_i} \cos\frac{\phi}{2} \left[1 - \frac{2}{3} X_i^2 \right] \\ &= -\Pi_{ii}^{32}(\vec{q}, \Omega) \end{aligned} \quad (6)$$

where $L_i = \ln\left(\frac{2\Lambda}{\Delta_i}\right)$ and $X_i^2 = -\left(\frac{\Omega}{2\Delta_i}\right)^2 + \frac{v_F^2}{2} \left(\frac{q}{2\Delta_i}\right)^2$.

It is intuitive to reexpress Eq. 4 as

$$\begin{aligned} 2 \sum_j (u^{-1})_{ij} \delta_j^a &= 2 \sum_j (u^{-1})_{ij} \delta_j^a(0) + \sum_b \Pi_{ii}^{a,b} \delta_i^b \\ 2\delta\rho &= - \sum_j 2N_0V(q) [\Pi_{jj}^{31}\delta_j^R - \Pi_{jj}^{32}\delta_j^I + \Pi_{jj}^{33}\delta\rho] \end{aligned} \quad (7)$$

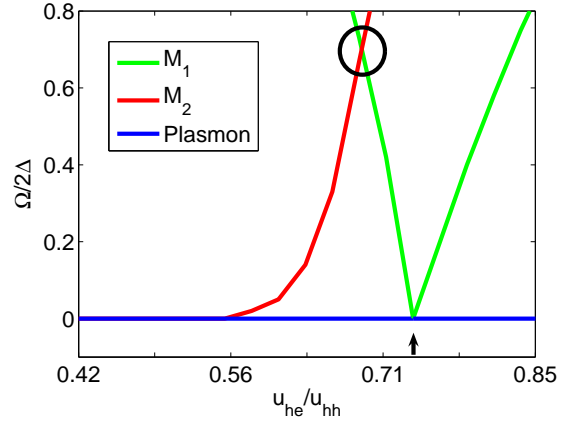


FIG. 4: Doping evolution of the frequencies of the relevant collective modes at $q=0$. The plasmon mode frequency vanishes at $q=0$ for all u_{he} . Mode M_1 describes relative phase fluctuation of the two hole gaps. It softens^{20,21,23} at the transition point between $++$ and TRSB states (at $u_{he} = u_{he}^{max}$, indicated by the arrow). Mode M_2 describes coupled antisymmetric phase fluctuation of the two hole gaps and longitudinal fluctuation of the electron gap. This mode lies below twice the energy of the electron gap and softens at the boundary between TRSB and $+-$ states, at $u_{he}^{min} = 0$. Numerically, the energy of the M_2 mode becomes small already for $u_{he} \leq u_{he}^{max}$ because electron gap rapidly decreases with decreasing u_{he} . The circle represents the case discussed in Ref. 23.

where $\delta_i^b = (\delta_i^R, -\delta_i^I, \delta\rho)$. This 7×7 set can be cast into the form

$$\underline{K}(q, \Omega) \vec{\delta} = \underline{u}^{-1} \vec{\delta}(0) \quad (8)$$

where $\vec{\delta}$ is a 7-component vector with elements $\delta_i^R, -\delta_i^I, \delta\rho$ ($\vec{\delta}(0)$ is the bare vertex),

$$\underline{u}^{-1} = \begin{pmatrix} \frac{1}{u_{hh}} & -\frac{1}{u_{hh}} & -\frac{1}{u_{he}} & 0 & 0 & 0 & 0 \\ -\frac{1}{u_{hh}} & \frac{1}{u_{hh}} & -\frac{1}{u_{he}} & 0 & 0 & 0 & 0 \\ -\frac{1}{2u_{he}} & -\frac{1}{2u_{he}} & -\frac{1}{2u_{he}^2} & 0 & 0 & 0 & 0 \\ 0 & 0 & 0 & \frac{1}{u_{hh}} & -\frac{1}{u_{hh}} & -\frac{1}{u_{he}} & 0 \\ 0 & 0 & 0 & -\frac{1}{u_{hh}} & \frac{1}{u_{hh}} & -\frac{1}{u_{he}} & 0 \\ 0 & 0 & 0 & -\frac{1}{2u_{he}} & -\frac{1}{2u_{he}} & -\frac{1}{2u_{he}^2} & 0 \\ 0 & 0 & 0 & 0 & 0 & 0 & 0 \end{pmatrix}, \quad (9)$$

and

$$\underline{K}(q, \Omega) = \begin{pmatrix} \frac{1}{u_{hh}} + \Pi_{h_1 h_1}^{11} & -\frac{1}{u_{hh}} & -\frac{1}{u_{he}} & -\Pi_{h_1 h_1}^{12} & 0 & 0 & \Pi_{h_1 h_1}^{13} \\ -\frac{1}{u_{hh}} & \frac{1}{u_{hh}} + \Pi_{h_2 h_2}^{11} & -\frac{1}{u_{he}} & 0 & -\Pi_{h_2 h_2}^{12} & 0 & \Pi_{h_2 h_2}^{13} \\ -\frac{1}{2u_{he}} & -\frac{1}{2u_{he}} & -\frac{1}{2u_{he}^2} + \Pi_{ee}^{11} & 0 & 0 & -\Pi_{ee}^{12} & \Pi_{ee}^{13} \\ -\Pi_{h_1 h_1}^{21} & 0 & 0 & \frac{1}{u_{hh}} + \Pi_{h_1 h_1}^{22} & -\frac{1}{u_{hh}} & -\frac{1}{u_{he}} & -\Pi_{h_1 h_1}^{23} \\ 0 & -\Pi_{h_2 h_2}^{21} & 0 & -\frac{1}{u_{hh}} & \frac{1}{u_{hh}} + \Pi_{h_2 h_2}^{22} & -\frac{1}{u_{he}} & -\Pi_{h_2 h_2}^{23} \\ 0 & 0 & -\Pi_{ee}^{21} & -\frac{1}{2u_{he}} & -\frac{1}{2u_{he}} & -\frac{1}{2u_{he}^2} + \Pi_{ee}^{22} & -\Pi_{ee}^{23} \\ \Pi_{h_1 h_1}^{31} & \Pi_{h_2 h_2}^{31} & 2\Pi_{ee}^{31} & -\Pi_{h_1 h_1}^{32} & -\Pi_{h_2 h_2}^{32} & -2\Pi_{ee}^{32} & M \end{pmatrix} \quad (10)$$

Here $M = -\frac{1}{N_0 V_q} + \Pi_{h_1 h_1}^{33} + \Pi_{h_2 h_2}^{33} + 2\Pi_{ee}^{33}$.

The dispersions of seven collective excitations are obtained from the condition $\text{Det} \underline{K}(q, \Omega) = 0$.

To adequately describe the full spectrum of all long-wavelength collective modes, one has to expand in $v_F q / \Delta$, but allow frequency to be of order of Δ (see Ref. 46 and Appendix C). Our goal, however, is limited: we want to find the plasmon mode in 2D and the modes which soften at the boundaries of the TRSB state. All these modes are low-energy modes in the long-wavelength limit, and to capture them in our approach, it is sufficient to use double expansion in $v_F q / \Delta$ and in Ω / Δ . To get other modes (or resonances) one needs to search for frequencies around 2Δ .

In the $++$ state, $\phi = 0$ in equilibrium, and δ^I and δ^R describe phase and magnitude fluctuations, respectively. One can easily make sure (see Appendix C) that these two sets of fluctuations decouple and there are no solutions for amplitude fluctuations at $\Omega \ll \Delta$.

The three orthogonal phase modes are $\delta_a^I \equiv \delta_1^I - \delta_2^I$, $\delta_b^I \equiv \delta_1^I + \delta_2^I + (2/\gamma)\delta_3^I$, $\delta_c^I \equiv \delta_1^I + \delta_2^I - (2/\gamma)\delta_3^I$, where $\gamma = 2u_{he}L_0$ and $L_0 = \frac{u_{hh} + \sqrt{u_{hh}^2 + 16u_{he}^2}}{8u_{he}^2}$. The mode δ_b^I is gapped everywhere in the $++$ phase. The mode δ_c^I describes fluctuations of the overall phase. This mode is

coupled to fluctuations of the electron density $\delta\rho$ as

$$\begin{aligned} -\frac{i\Omega}{\Delta}\delta_c^I - \left(\frac{1}{N_0 V_q} + 8\right)\delta\rho &= 0 \\ \frac{v_F^2 q^2 - 2\Omega^2}{4\Delta^2}\delta_c^I + \frac{4i\Omega}{\Delta}\delta\rho &= 0 \end{aligned} \quad (11)$$

The corresponding dispersion is a 2D plasmon with $\Omega_{pl}^2 = \frac{v_F^2 q^2}{2}(8N_0 V_q + 1)$. Observe that the plasmon frequency remains the same as in the normal state⁴⁸. In general, Ω_{pl} in a superconductor scales with the density of superconducting electrons and is sensitive to disorder⁴³. In our case (clean limit), superconducting density coincides with the full electron density, hence Ω_{pl} does not change between normal and superconducting states.

The mode δ_a^I describes antisymmetric phase fluctuations of the gaps on the two hole pockets. The condensation of this mode signals the transition to the TRSB state. In the static limit, this mode totally decouples from density fluctuations. Near $u_{he} = u_{he}^{max}$ we obtained at $q = 0$, $(\Omega_{\delta_a^I}^2)^2 = (8\sqrt{2}/3)(2\Delta/u_{he}^{max})^2(u_{he} - u_{he}^{max})$. Not surprisingly, the antisymmetric phase mode softens at the transition point into the TRSB state (where $u_{he} = u_{he}^{max}$). We show the behavior of $\Omega_{\delta_a^I}^2$ in Fig.4). To properly obtain the dispersion of this mode, one has to do more involved calculations as the combinations of δ_1^I , δ_2^I , and δ_3^I , which decouple at a finite q , are not the same as at $q = 0$. As a result, the dispersions of Leggett-type modes generally depend on the Coulomb interaction^{21,41,44}.

Inside the TRSB state, phase and amplitude fluctuations get mixed up, as was noticed in Refs.21,23. This is easily seen from Eq. 10 as the off-diagonal components which connect the real and imaginary parts of the order parameter fluctuations, are given by Π^{12} which are proportional to $\sin \frac{\phi}{2}$ (see Eq. 6) and are non-zero once $\phi \neq 0, \pi$.

The mode which corresponds to the overall phase change is now $-(\delta_1^R - \delta_2^R) \sin \frac{\phi}{2} + (\delta_1^I + \delta_2^I) \cos \frac{\phi}{2} - \frac{2}{\gamma} \delta_3^I$, where in the TRSB state $\gamma = 2(u_{he}/u_{hh}) \cos \frac{\phi}{2}$, and ϕ is given by Eq. (3). This mode decouples from other phase and magnitude modes, but again couples to $\delta\rho$ and remains a 2D plasmon. We solved for the remaining modes and found that the mode $\delta_1^I - \delta_2^I$, which described antisymmetric phase fluctuations of Δ_{h_1} and Δ_{h_2} outside the TRSB region and softened at the upper boundary of the TRSB state, acquires a new functional form inside the TRSB state, and gets gapped, as expected. As u_{he} decreases and ϕ increases and approaches π , another mode, indicated as the M_2 mode in Fig.4, gets soft. This mode is a coupled oscillation of δ_3^R and $\delta_1^R + \delta_2^R$. The first describes longitudinal fluctuations of the electron gap, which vanishes at the lower boundary of TRSB state, the second describes antisymmetric phase fluctuations of the two hole gaps (for $\phi = \pi - 2\tilde{\phi}$ and $\tilde{\phi} \ll 1$, $\Delta_{h_1} \rightarrow \Delta e^{i(\frac{\pi}{2} - \tilde{\phi})} \approx \Delta(i + \tilde{\phi})$, and $\Delta_{h_2} \rightarrow \Delta e^{-i(\frac{\pi}{2} - \tilde{\phi})} \approx \Delta(-i + \tilde{\phi})$, and $\delta_2^R + \delta_1^R = 2\delta_2^R = 2\tilde{\phi}$ describes small deviations from the $+-$ state). The calculation of this mode requires some extra care because electron gap Δ_e vanishes at the lower boundary of TRSB state, and the expansion in $\Omega^2/(2\Delta_e)^2$ is only valid if the mode frequency is below $2\Delta_e$ (Ref.45). Using the formal expansion in Ω , we obtained the frequency of M_2 mode $\Omega_{M_2} = \sqrt{3}(2\Delta_e)$, which is outside the applicability limit of the expansion. A more accurate approach is to keep Ω along with Δ_e , i.e., replace $\Omega^2/(2\Delta_e)^2$ by $\Omega^2/(4\Delta_e^2 - \Omega^2)$. This gives $\Omega_{M_2} = (\sqrt{3}/2)(2\Delta_e)$, which is below the threshold at $2\Delta_e$. We also found another low-energy mode using the expansion in Ω , however its energy is above $2\Delta_e$ even when we keep Ω along with Δ_e . This excitation is then inside the continuum and is not a true collective mode.

We emphasize that the vanishing of Δ_e is a peculiarity of the minimal model. In a more general model, the TRSB state emerges from the modified $+-$ state, in which Δ_e is already non-zero. Then it is completely safe to search for soft modes by expanding in Ω/Δ_i .

III. BEYOND THE MINIMAL MODEL

We analyzed whether the TRSB state survives in more general cases. As a first step, we included intra-pocket density-density interactions u_{h_1} , u_{h_2} , and u_e . Applying the same procedure as before, we found that, for $u_{h_1} = u_{h_2}$, the phase diagram and the behavior of collective modes remain the same as in Figs.

1 and 4, the only modification is that at $T = 0$ the lower boundary of the TRSB state now shifts to a finite $u_{he}^{min} = \sqrt{\frac{u_e u_{hh}}{2}}$. The upper boundary becomes $u_{he}^{max} \approx u_{he}^0 \left[1 + \frac{u_{hh}}{4} \frac{(1 - \frac{u_{h_1}}{u_{hh}})^2}{\chi^2} \ln \left(\frac{2}{\chi} \right) \right]$, where $\chi = \left(\sqrt{1 - \frac{u_{h_1} - u_e}{u_{hh}}} \right)$ and $u_{he}^0 = \frac{u_{hh}}{\sqrt{2}} \chi$ is the point at which TRSB state emerges right at T_c .

When $u_{h_1} \neq u_{h_2}$, the phase diagram changes qualitatively (see Fig. 1 b). Now one of the hole gaps continuously evolves from negative to positive along the T_c line, passing through zero in between (see Appendix A for details). The TRSB state still emerges, but at a lower T , and survives as long as intra-pocket interactions remain small compared to u_{hh} (see Appendix B). To simplify the presentation, we consider the representative case when $u_{h_2}, u_e = 0$ and $u_{h_1} \ll u_{hh}$ to understand the changes to the phase diagram. The phase diagram for a generic $u_{h_1} \neq u_{h_2}$ is qualitatively the same as in the case we considered.

We found that TRSB state at $T = 0$ now exists in an interval between $u_{he}^{min} = 0$ and $u_{he}^{max} \approx \frac{u_{hh}}{\sqrt{2}} \left(1 - \frac{u_{hh}}{4} \ln \left[2/(1 + e^{-u_{h_1}/u_{hh}^2}) \right] \right)$.

We also considered anisotropic inter-pocket interaction u_{hh} with an extra $\cos 4\theta$ term, consistent with lattice symmetry¹¹. This gives rise to $\cos 4\theta$ angular variations of Δ_{h_1} and Δ_{h_2} and may lead to accidental gap nodes. The solution of the set of the gap equations for $u_{h_1} \neq u_{h_2}$ and $u_{hh}(\theta) = u_{hh}(1 + \alpha(\cos \theta_{h_1} + \cos \theta_{h_2}))$ is quite involved. However, one can show quite generally that TRSB state is confined to low temperatures and is separated from the T_c line, like we previously had for angle-independent interactions. Immediately below T_c , the $+-$ state gradually evolves into $++$ state, however, now only the average value of the “minus” gap goes through zero at some intermediate u_{he} , while the gap itself does not vanish and just oscillates along the corresponding pocket. We illustrate this in Fig 5.

Inside the TRSB state at $T < T_c$, the number of coupled gap equations equals to nine because in general $\Delta_{h_i} = \Delta_i (e^{i\phi_{ia}} + r_i e^{i\phi_{ib}} \cos 4\theta_1)$, $i = 1, 2$. For $u_{h_1} = u_{h_2}$, we find that $\Delta_{h_1} = \Delta_{h_2}^* = \Delta e^{i\phi/2} (1 + (r_a e^{-i\phi} + r_b) \cos 4\theta_1)$. For $\phi = 0$ (the $++$ state), accidental nodes exist if $|r_a + r_b| > 1$, for $\phi = \pi$ (the $+-$ state), they exist if $|r_a - r_b| > 1$. In the TRSB state, however, $|\Delta_{h_i}|$ doesn't cross zero and can only have gap minima. We illustrate this behavior in Fig. 6 for the experimentally relevant case when $+-$ state is nodal and $++$ state has a full gap. Observe that the distance between deep minima gets larger upon entering the TRSB state. This behavior is consistent with recent laser ARPES studies of doped $\text{Ba}_{1-x}\text{K}_x\text{Fe}_2\text{As}_2$ (Ref.32).

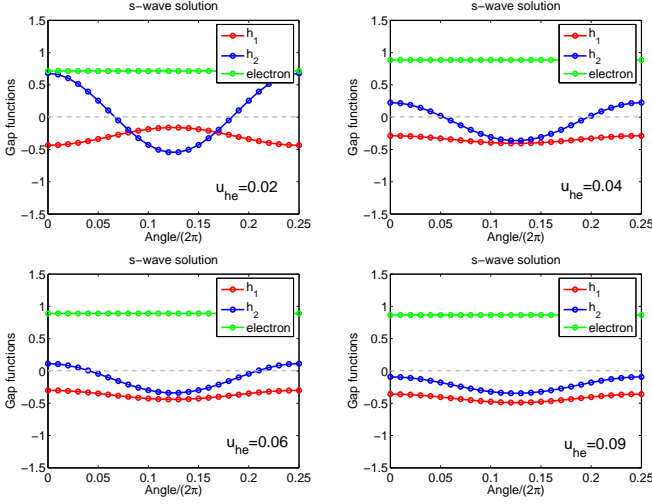


FIG. 5: The $+-$ to $++$ transition at T_c , with increasing u_{he} for the case when the two hole pockets are not equivalent and the interaction u_{hh} has $\cos 4\theta$ angular dependence. The solutions of the linearized gap equations are shown for $u_{he} = 0.02, u_{he} = 0.04, u_{he} = 0.06, u_{he} = 0.09$ from left to right and top to bottom, respectively. Other parameters are $\alpha = 0.05, u_{h1} = 0.2, u_{h2} = 0.26, u_{hh} = 0.2$. Note how one of the hole gap's average value gets smaller as u_{he} increases, goes through zero, and reappears with the opposite sign and with small angular variation at larger u_{he} . We expect such behavior immediately below T_c line in $\text{Ba}_{1-x}\text{K}_x\text{Fe}_2\text{As}_2$, as x decreases from one.

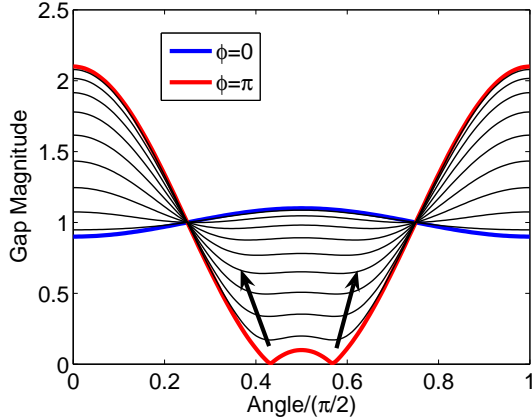


FIG. 6: The gap evolution in the TRSB state for angle-dependent interactions and two equivalent GCP's, in a situation when the gap in $+-$ state has accidental nodes and the gap in $++$ state is nodeless. The nodes disappear once the system enters the TRSB state, but deep minima (shown by arrows) remain in some range of ϕ (or equivalently u_{he}).

IV. CONCLUSIONS

We considered the evolution of the superconducting gap structure in strongly hole doped $\text{Ba}_{1-x}\text{K}_x\text{Fe}_2\text{As}_2$. Near optimal doping ($x \sim 0.4$) the pairing symmetry is s_{\pm} , with different gap sign on hole and electron pock-

ets, but the same sign of the gap on the hole pockets (a $++$ state in our terminology). In pure KFe_2As_2 ($x = 1$), which has only hole pockets, there are experimental and theoretical arguments for both d -wave and s -wave gap, the latter changes sign between the two GCP's (a $+-$ state). We assumed s -wave gap symmetry for KFe_2As_2 , consistent with the laser ARPES data³⁴. The issue we addressed is how a $++$ gap on the GCP's transforms into a $+-$ gap as $x \rightarrow 1$. We found that, for identical GCP's, there is critical point along T_c line at which the system jumps from $+-$ to $++$ state (see Fig. 1a). At a lower T , the transformation occurs via an intermediate $s + is$, state in which the gaps on the two GCP's differ in phase by ϕ which gradually involves from $\phi = \pi$ on one end (the $+-$ state) to $\phi = 0$ on the other end (the $++$ state). The system spontaneously chooses either ϕ or $-\phi$ and with this choice breaks time-reversal symmetry. We computed the dispersion of collective excitations and found that two Leggett-type modes soften at the two ends of the TRSB state. We found that the TRSB state survives even when the two GCP's are non-identical and also when the gap on hole pockets is angle-dependent, and even when $+-$ and/or $++$ states have accidental gap nodes. In the former case, near T_c the system gradually evolves from the $+-$ to $++$ state, but the TRSB state still emerges at a lower T (see Fig. 1b). In the second, the nodes get lifted once the system enters into a TRSB state (but deep minima remain). The $s + is$ state is not chiral, but e.g., Kerr effect measurements still should be able to detect the breaking of time-reversal symmetry. These measurements are clearly called for.

We acknowledge stimulating conversations with L. Benfatto, R. Fernandes, I. Eremin, A. Finkelstein, P. Hirschfeld, A. Kamenev, M. Khodas, A. Levchenko, Y. Matsuda, I. Mazin, R. Prozorov, J.P. Reid, T. Shibauchi, V. Stanev, L. Taillefer, R. Thomale, V. Vakaryuk, and M. Vavilov. We are particularly thankful to L. Benfatto for pointing out an error in our original calculation of the collective modes near the lower boundary of TRSB state. The research has been supported by DOE DE-FG02-ER46900. SM also acknowledges support from ICAM-DMR-084415.

Appendix A: The Free Energy

We follow a standard procedure and introduce bosonic fields Δ_{h1}, Δ_{h2} , and Δ_e , which describe fluctuations of the superconducting order parameters on the two hole and one electron pockets. We decouple four-fermion interactions using a Hubbard-Stratonovic(HS) transformation, integrate over fermions, obtain $Z = \int d\Delta_i e^{-\mathcal{F}[\Delta_i]}$, and analyze $\mathcal{F}[\Delta_i]$ in the saddle-point approximation. For a model with intra-pocket and inter-pocket interactions within hole pockets (u_{h1}, u_{h2} and u_{hh} terms, respectively) and the interaction between hole and electron

pockets (u_{he} term), we obtained

$$\begin{aligned} \mathcal{F}[\Delta_i] = & -\frac{1}{2u_{hh} - u_{h_1} - u_{h_2}} [-2(|\Delta_{h_1}|^2 + |\Delta_{h_2}|^2) + \\ & + 2(\Delta_{h_1}\Delta_{h_2}^* + \Delta_{h_1}^*\Delta_{h_2}) \\ & + \frac{2(u_{hh} - u_{h_2})}{u_{he}} (\Delta_{h_1}\Delta_e^* + \Delta_{h_1}^*\Delta_e) \\ & + \frac{2(u_{hh} - u_{h_1})}{u_{he}} (\Delta_{h_2}\Delta_e^* + \Delta_{h_2}^*\Delta_e) \\ & + \frac{2(u_{h_1}u_{h_2} - u_{hh}^2)}{u_{he}^2} |\Delta_e|^2] \\ & - 2L \sum_x |\Delta_x|^2 + \int G^2 \tilde{G}^2 \sum_x |\Delta_x|^4 \end{aligned} \quad (\text{A1})$$

where $L \equiv \int G \tilde{G} \sim \ln \frac{2\Lambda}{T}$, the sum over x runs over two hole and two electron pockets, and $G = (i\omega - \varepsilon)^{-1}$ and $\tilde{G} = (i\omega + \varepsilon)^{-1}$.

Let us first consider the case $u_{h_1} = u_{h_2} = 0$. Then one can diagonalize the quadratic part of the Free energy by introducing

$$\begin{aligned} \phi_1 &= \cos \Theta \frac{\Delta_{h_1} + \Delta_{h_2}}{2} - \sin \Theta \Delta_e \\ \phi_2 &= \sin \Theta \frac{\Delta_{h_1} + \Delta_{h_2}}{2} + \cos \Theta \Delta_e \\ \phi_3 &= \frac{\Delta_{h_1} - \Delta_{h_2}}{2} \end{aligned} \quad (\text{A2})$$

where $\cos \Theta = 1/\sqrt{1 + \zeta^2}$, $\sin \Theta = \zeta/\sqrt{1 + \zeta^2}$, and $\zeta = \frac{u_{hh}}{4u_{he}} \left(1 + \sqrt{1 + \frac{16u_{he}^2}{u_{hh}^2}}\right)$. The action in terms of ϕ_i takes the form

$$\Delta \mathcal{F}_{(2)}[\phi_i] = \lambda_1 |\phi_1|^2 + \lambda_2 |\phi_2|^2 + \lambda_3 |\phi_3|^2, \quad (\text{A3})$$

where

$$\begin{aligned} \lambda_1 &= \frac{u_{hh}}{2u_{he}^2} \left(1 + \sqrt{1 + \frac{16u_{he}^2}{u_{hh}^2}}\right) - 4L \\ \lambda_2 &= \frac{u_{hh}}{2u_{he}^2} \left(1 - \sqrt{1 + \frac{16u_{he}^2}{u_{hh}^2}}\right) - 4L \\ \lambda_3 &= \frac{4}{u_{hh}} - 4L \end{aligned} \quad (\text{A4})$$

Since λ_2 is strongly negative, the HS transformation for ϕ_2 does not make sense. Because this field does not condense on physics grounds, we just set $\phi_2 = 0$ (see Ref. 49 for more discussion on this). The two other λ 's change sign at some, generally different, temperatures, which depend on u_{he}/u_{hh} . When this happens, either ϕ_1 or ϕ_3 condense, depending on whether λ_1 or λ_3 changes sign first upon lowering T , i.e., increasing L . (This procedure is formally equivalent to diagonalizing the linearized gap equation to identify the state with the leading eigenvalue

which in this case would correspond to either the field ϕ_1 or ϕ_3 .) The condensation of ϕ_1 , with $\phi_2 = \phi_3 = 0$ brings the system into a $++$ phase ($\Delta_{h_1} = \Delta_{h_2} = -\Delta_e/\gamma$), while the condensation of ϕ_3 with $\phi_2 = \phi_1 = 0$ brings the system into a $+ -$ phase ($\Delta_{h_1} = -\Delta_{h_2}$, $\Delta_e = 0$). At $u_{he} = u_{hh}/\sqrt{2}$, λ_1 and λ_2 reach zero at the same T , and ϕ_1 and ϕ_3 condense simultaneously (for this u_{he} , $\cos \Theta = 1/\sqrt{3}$). The relative magnitude and the relative phase between ϕ_1 and ϕ_3 are decided by minimizing the quartic terms in the Free energy. Plugging in Δ_i in terms of ϕ_i into Eq. A1, neglecting ϕ_2 , and using $u_{he} = u_{hh}/\sqrt{2}$ we obtain

$$\Delta \mathcal{F}_{(4)}[\phi_i] = K_1 (|\phi_1|^2 + |\phi_3|^2)^2 + K_2 |\phi_1^2 + \phi_3^2|^2 + K_3 |\phi_1|^4 \quad (\text{A5})$$

where $K_1 = \frac{C}{3}$, $K_2 = \frac{C}{6}$, $K_3 = -\frac{2C}{9}$, and $C > 0$. The K_1 term is isotropic, the K_3 term depends on the relative magnitudes of ϕ_1 and ϕ_3 fields, and the K_2 term $K_2 |\phi_1^2 + \phi_3^2|^2 = K_2 (|\phi_1|^4 + |\phi_3|^4 + 2|\phi_1|^2 |\phi_3|^2 \cos 2\theta)$. depends on the relative magnitude and the relative phase θ between ϕ_1 and ϕ_3 : A positive K_2 (our case) selects $\theta = \pm\pi/2$, i.e., if one condensate is real, another is purely imaginary. Solving for the amplitudes we find $|\phi_3|^2 = |\phi_1|^2 (1 + K_3/2K_2) = |\phi_1|^2/3$. The state in which both ϕ_1 and ϕ_3 are present, and the relative phase is not 0 or π is our TRSB state. Eq. A5 is presented in the main text with $\phi_1 \rightarrow a$ and $\phi_3 \rightarrow b$.

Away from the degeneracy point the quadratic part of the free energy takes the form

$$\mathcal{F}_{(2)}[\phi_i] = \left(\lambda + \frac{16}{3} \frac{x}{u_{hh}}\right) |\phi_1|^2 + \lambda |\phi_3|^2 \quad (\text{A6})$$

where $\lambda = 4(1/u_{hh} - L)$ and $x = 1 - \sqrt{2}u_{he}/u_{hh}$. The leading instability to the left of the degeneracy point (at $x > 0$) is into the ϕ_3 state, and to the right of it (at $x < 0$) it is into the ϕ_1 state. Once one order sets in, it acts against the appearance of the other. Still, we found that, e.g., at $x > 0$, ϕ_1 still condenses at $\lambda_{cr} = -(16x/3u_{hh})((K_1 + K_2)/2K_2) = -(16x/3u_{hh}) * (3/2)$. The corresponding temperature T_{cr} is smaller than without K terms, but is still finite. Once ϕ_1 becomes non-zero, a positive K_2 again selects a relative phase of $\pm\pi/2$ between ϕ_3 and ϕ_1 (which corresponds to the $\phi = \pi$ boundary for the TRSB state). This consideration leads to the phase diagram in Fig. 1a in the main text.

We extended this analysis to the case when $u_{h_1} = u_{h_2} \neq 0$ and found the same results as above. However, when $u_{h_1} \neq u_{h_2}$, the phase diagram changes qualitatively. To show the new physics and at the same time avoid lengthy formulas, we set $u_{h_1} \ll u_{hh}$; $u_{h_2} = 0$ and consider u_{he} near $u_{hh}/\sqrt{2}$, at which $++$ and $+ -$ phases cross at T_c . Specifically, we set $u_{h_1} = 2yu_{hh}$, $u_{he}^2 = (u_{hh}^2/2)(1 + 2cy)$, and obtained the phase diagram to first order in $y \ll 1$.

At a non-zero y , the quadratic part of the Free energy

reads

$$\begin{aligned}\mathcal{F}_2[\phi_i] = & 4 \left(\frac{1+y(1-4c)/3}{u_{hh}} - L \right) |\phi_1|^2 \\ & + 4 \left(\frac{1+y}{u_{hh}} - L \right) |\phi_3|^2 \\ & - 4 \left(\frac{1+y(7-10c)/3}{2u_{hh}} + L \right) |\phi_2|^2 \\ & - \frac{2\sqrt{2}y}{\sqrt{3}u_{hh}} \left(\phi_3^*(\phi_2 - \sqrt{2}\phi_1) + c.c \right) \quad (\text{A7})\end{aligned}$$

The ϕ_2 mode is again non-critical, and ϕ_2 can be sent to zero. For the remaining two modes, we have

$$\begin{aligned}\mathcal{F}_2[\phi_i] = & 4 \left(\frac{(1+y)}{u_{hh}} - L \right) |\phi_3|^2 \\ & + 4 \left(\frac{1+y(1-4c)/3}{u_{hh}} - L \right) |\phi_1|^2 \\ & + \frac{4y}{\sqrt{3}u_{hh}} (\phi_3\phi_1^* + c.c) \quad (\text{A8})\end{aligned}$$

Diagonalizing this quadratic form by

$$\phi_1 = \psi_1 \cos \eta + \psi_3 \sin \eta \quad \phi_3 = -\psi_1 \sin \eta + \psi_3 \cos \eta, \quad (\text{A9})$$

we obtain $\tan 2\eta = \sqrt{3}/(1+2c)$. Taking the positive root $\tan \eta = \frac{1}{\sqrt{3}} \left[\sqrt{(1+2c)^2 + 3} - (1+2c) \right]$, we obtain

$$\begin{aligned}\mathcal{F}_2[\psi_i] = & 4 \left[\left(\frac{1 + \frac{y}{3} \left(2(1-c) - \sqrt{(1+2c)^2 + 3} \right)}{u_{hh}} - L \right) |\psi_1|^2 \right. \\ & \left. + \left(\frac{1 + \frac{y}{3} \left(2(1-c) + \sqrt{(1+2c)^2 + 3} \right)}{u_{hh}} - L \right) |\psi_3|^2 \right] \quad (\text{A10})\end{aligned}$$

We see that the temperatures at which ψ_1 and ψ_3 modes condense are different and ψ_1 mode condenses first for all values of c . The ψ_1 mode condenses at $L_{\psi_1} = (1+S_1(c))/u_{hh}$, where $S_1(c) = (8/3)(1-c-\sqrt{1+c+c^2})$, and the ψ_3 mode condenses at $L_{\psi_3} = (1+S_3(c))/u_{hh}$, where $S_3(c) = (8/3)(1-c+\sqrt{1+c+c^2})$. We plot the temperatures at which the prefactors for $|\psi_1|^2$ and $|\psi_3|^2$ terms vanish in Fig 7. The condensation of ψ_1 field leads to a superconducting state in which all three gaps Δ_{h_1} , Δ_{h_2} , and Δ_e are generally present and are different from each other. At large positive c (i.e., at larger u_{he}) the state immediately below the condensation temperature of ψ_1 is close to the $++$ state, with $\Delta_{h_1} \approx \Delta_{h_2}$ and Δ_e of opposite sign compared to Δ_{h_1} and Δ_{h_2} . At large negative c (smaller u_{he}) the state immediately below the condensation temperature of ψ_1 is close to the $+-$ state, with $\Delta_{h_1} \approx -\Delta_{h_2}$ and smaller Δ_e . In between, the condensed state is a mixture of $++$ and $+-$ states. In particular, for $c = 0$, $\Delta_e = -\Delta_{h_2}/\sqrt{2}$ and $\Delta_{h_1} = 0$, i.e., the

gap on the hole pocket, for which we kept intra-pocket repulsion, vanishes. We analyzed the form of the condensate for various c (i.e., various u_{he}/u_{hh}) and found a continuous evolution, in the process of which one of hole gaps gets smaller, passes through zero, and then re-emerges with the opposite sign. Specifically, we found, right below T_c for the ψ_1 mode,

$$\begin{aligned}\Delta_e = & -\frac{\Delta_{h_1} + \Delta_{h_2}}{\sqrt{2}}, \\ \frac{\Delta_{h_1} - \Delta_{h_2}}{\Delta_{h_1} + \Delta_{h_2}} = & (1+2c) - \sqrt{3 + (1+2c)^2} \quad (\text{A11})\end{aligned}$$

Without quartic terms, the modes ψ_1 and ψ_3 are decoupled and the system undergoes two superconducting transitions at L_{ψ_1} and L_{ψ_3} . The mode which condenses at L_{ψ_3} is almost $++$ state at large negative c , almost $+-$ state at large positive c , and a mixed state in between. E.g., at $c = 0$, the ψ_3 condensate has components $\Delta_{h_1} = -2\Delta_{h_2}$, $\Delta_e = \Delta_{h_2}/\sqrt{2}$.

The situation changes when we include quartic terms into consideration. We use Eq. (A5) as an input, substitute $\phi_{1,3}$ in terms of $\psi_{1,3}$ via (3), and obtain $\mathcal{F}_4[\psi_i]$. Carrying out the calculations, we find that the four-fold term contains a linear piece in ψ_3 in the form $2K_3 \sin 2\eta \cos^2 \eta |\psi_1|^3 |\psi_3| \cos \theta_{13}$, where θ_{13} is a relative phase between the condensates of ψ_1 and ψ_3 . This term acts as an "external field" for ψ_3 and makes ψ_3 non-zero once ψ_1 condenses. Because $K_3 < 0$, the system initially selects $\theta_{13} = 0$, i.e., ϕ_3 field emerges with the same phase as ϕ_1 . This implies that the state immediately below L_{ψ_1} breaks a $U(1)$ gauge symmetry (the overall phase gets fixed), but time-reversal symmetry remains unbroken. The situation changes, however, when the temperature gets lower and ψ_3 grows. The full dependence of $\mathcal{F}_4[\psi_i]$ on θ_{13} is in the form

$$\begin{aligned}\mathcal{F}_4[\psi_i] = & 2K_3 \cos \theta_{13} \sin 2\eta \\ & \times |\psi_1| |\psi_3| (|\psi_1|^2 \cos^2 \eta + |\psi_3|^2 \sin^2 \eta) \\ & + \cos^2 \theta_{13} |\psi_1|^2 |\psi_3|^2 (4K_2 + K_3 \sin^2 2\eta) \quad (\text{A12})\end{aligned}$$

Analyzing this form, we immediately find that the prefactor for $\cos^2 \theta_{13}$ is necessary positive. Minimizing with respect to θ_{13} , we then find that, at some finite ψ_3 , the equilibrium value of θ_{13} shifts from $\phi_{13} = 0$ to a finite $\theta_{13} = \pm b$, $b \neq 0$. For large and small c , this happens already at small ψ_3 , which are well within the applicability of the expansion in powers of ψ . Thus, for large positive c , the critical $|\psi_3| = |\psi_1|/(\sqrt{3}|1+2c|)$.

Once the system selects a non-zero θ_{13} , it breaks additional Z_2 symmetry by selecting either positive or negative value of the relative phase θ_{13} . The Z_2 breaking then implies that time-reversal symmetry is broken, i.e., once θ_{13} becomes non-zero, the system enters into a TRSB phase. The region of this phase shrinks as u_{h_1} increases but definitely remains finite as long as $u_{h_1} \ll u_{hh}$, i.e., as long as our parameter y is small.

When both u_{h_1} and u_{h_2} are non-zero, the calculations become more involved, but the physics remains the same.

We also analyzed the effect of adding intra-pocket interaction u_e for electron pockets. Like in the case of $u_{h_1} = u_{h_2}$, a non-zero u_e shifts the lower boundary of the TRSB state to a finite u_{he} . There is one new effect compared to the case $u_{h_1} = u_{h_2}$: because now (when $u_{h_1} \neq u_{h_2}$), Δ_e remains non-zero to the left of the lower boundary of the TRSB state, the mode which describes longitudinal fluctuations of Δ_e , no longer strongly couples to antisymmetric phase fluctuations of the two hole gaps, and the mode which softens at the lower boundary of TRSB state becomes a pure Leggett-type phase mode.

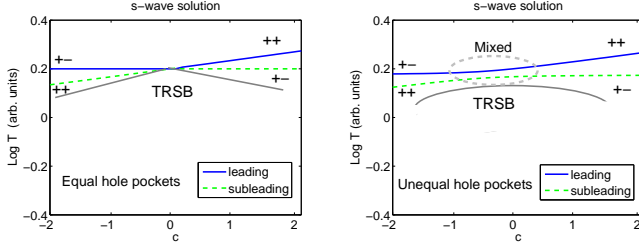


FIG. 7: Temperatures (T) at which the prefactors for the quadratic terms in Ginzburg-Landau expansion for the two critical fields change sign. The parameter c measures the deviation of hole-electron interaction u_{he} from the critical value ($= u_{hh}/\sqrt{2}$). Left panel – two equivalent hole pockets ($y = 0$). In this situation, the condensation of one critical field leads to $+-$ order, the condensation of the other leads to $++$ order. The two lines cross at the critical u_{he} . In the presence of mode-mode coupling, the emergence of one order tends to prevent the emergence of the other, and the actual temperature, at which the second order emerges, gets smaller (black line). We found (see text) that below the black line the two orders lock into TRSB state. Right panel – non-equivalent hole pockets ($y = 1/8$). The eigenfunctions reduce to pure $+-$ and $++$ only at large $|c|$, while in the region labeled ‘mixed’ the system gradually transforms from the $+-$ to $++$ order with one of the hole gaps going through zero in between. The lines at which the prefactors for the quadratic terms vanish now do not cross. Due to mode-mode coupling, the order which appears first now induces second order, i.e., both are present immediately below the actual T_c line, with a relative phase of 0 or π , i.e., time-reversal symmetry is not broken at T_c . The TRSB state still emerges, but at a lower T (below the black line).

Appendix B: Non-linear gap equations at $T = 0$

The key goal of the analysis is to show that TRSB state, which starts as a point along T_c line, extends to a finite range of system parameters at $T = 0$

The set of non-linear gap equations in a generic model with inter-pocket interactions u_{hh} , u_{he} , and intra-pocket interactions u_{h_1} , u_{h_2} , and u_e is shown diagrammatically in Fig 8. Each anomalous vertex is a gap Δ_x , which, in general, is a complex variable ($x = h_1, h_2$, and e), and each fermionic bubble is a sum of normal and anomalous

Green functions

$$G_{\alpha\beta}^{(x)} = -\delta_{\alpha,\beta} \frac{i\omega + \varepsilon_x}{\omega^2 + E_x^2}, \quad F_{\alpha\beta}^{(x)} = g_{\alpha,\beta} \frac{\Delta_x}{\omega^2 + E_x^2} \quad (B1)$$

where $E_x = \sqrt{\epsilon_x^2 + |\Delta_x|^2}$, ϵ_x is the fermionic dispersion near the pocket x , and $g_{\alpha,\beta} = i\sigma_{\alpha\beta}^y$. Evaluating the diagrams, we obtain at $T = 0$

$$\begin{aligned} \Delta_{h_1} &= -u_{h_1} \Delta_{h_1} L_1 - u_{hh} \Delta_{h_2} L_2 - 2u_{he} \Delta_e L_e \\ \Delta_{h_2} &= -u_{hh} \Delta_{h_1} L_1 - u_{h_2} \Delta_{h_2} L_2 - 2u_{he} \Delta_e L_e \\ \Delta_e &= -u_{he} \Delta_{h_1} L_1 - u_{he} \Delta_{h_2} L_2 - u_e \Delta_e L_e \end{aligned} \quad (B2)$$

where $L_x \equiv \ln \left(\frac{2\Lambda}{|\Delta_x|} \right)$

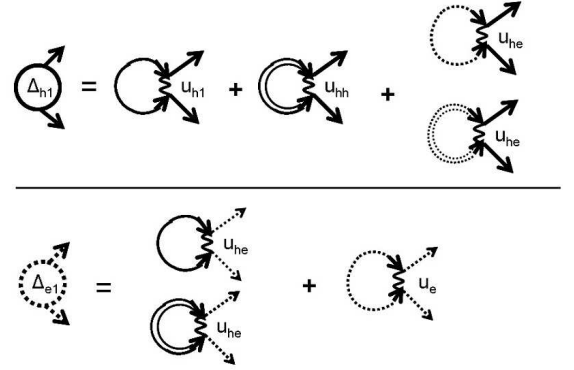


FIG. 8: Diagrammatic representation of the set of non-linear equations for the gaps Δ_{h_1} and Δ_{e_1} (viewed as anomalous self energies). In our case $\Delta_{e_1} = \Delta_{e_2} \equiv \Delta_e$. The equation for Δ_{h_2} is similar and not shown. The double headed arrows correspond to the anomalous Greens functions; The single and double solid lines and the single and double dotted lines are anomalous Green functions for fermions near the hole pockets ($h_{1,2}$) and near electron pockets ($e_{1,2}$), respectively.

1. The symmetric case

Consider first the symmetric case $u_{h_1} = u_{h_2}$. Then $\Delta_{h_1} = \Delta_{h_2} = \Delta$ and $L_1 = L_2 = L$. Without loss of generality, the overall phase can be set such that Δ_e is real. The two hole gaps must then satisfy $\Delta_{h_2} = \Delta_{h_1}^*$, i.e in general $\Delta_{h_1} = \Delta e^{i\phi/2}$, $\Delta_{h_2} = \Delta e^{-i\phi/2}$. The electron gap Δ_e also scales with Δ , and we write $\Delta_e = -\gamma\Delta$, in which case $L_e \equiv L - \ln\gamma$. The three variables Δ , γ , and ϕ are the solutions of the set of three non-linear gap equations (we recall that $L = \log \frac{2\Lambda}{\Delta}$). We have, from (Eq. B2),

$$\begin{aligned} [1 - (u_{hh} - u_{h_1}) L] \sin(\phi/2) &= 0 \\ [1 + (u_{hh} + u_{h_1}) L] \cos(\phi/2) &= 2u_{he} \gamma L_e \\ [1 + u_e L_e] \gamma &= 2u_{he} \cos(\phi/2) L \end{aligned} \quad (B3)$$

For the $+-$ state, $\phi = \pi$, and we have $\gamma = 0$ and $L = 1/(u_{hh} - u_{h1})$. For the $++$ state, $\phi = 0$, L is approximately the smallest positive solution of

$$1 + (u_e + u_{hh} + u_{h1})L + (u_e(u_{hh} + u_{h1}) - 4u_{he}^2)L^2 = 0 \quad (B4)$$

and γ is the solution of $\gamma(1 + u_e(L - \log \gamma)) = 2u_{he}L$.

For the TRSB state, ϕ is different from 0 and π , and we have

$$\begin{aligned} L &= \frac{1}{u_{hh} - u_{h1}} \\ L_e &= \frac{u_{hh}}{2u_{he}^2 - u_e u_{hh}} \\ \gamma &= 2 \frac{u_{he}L}{1 + u_e L_e} \cos \frac{\phi}{2} \end{aligned} \quad (B5)$$

The upper and lower boundaries of the TRSB state are obtained by matching the TRSB solution and the solutions for the $++$ and $+-$ states, respectively. This gives u_{he}^{max} and u_{he}^{min} , which we presented in the main text.

2. Non equivalent hole pockets

For $u_{h1} \neq u_{h2}$, $\Delta_{hi} = \Delta_i e^{i\phi_i/2}$, and both $\Delta_{1,2}$ and $\phi_{1,2}$ are generally different. The analysis now involves five variables (two complex Δ_{hi} an one real Δ_e , and is quite involved. However, less efforts are needed to just prove that TRSB state exists because near its upper and lower boundaries ϕ_1 and ϕ_2 approach zero or differ by π , respectively, and one can expand in the deviations from equilibrium ϕ_i 's.

As an example, consider the system near the upper boundary of the TRSB state. Here ϕ_1 and ϕ_2 are both small. Expanding in the set of complex equations (B2) for Δ_{hi} and Δ_e to linear order in $\phi_{1,2}$, and separating real and imaginary parts, we obtain, from the imaginary parts,

$$\begin{aligned} \Delta_1 (1 + u_{h1}L_1) \phi_1 + L_2 \Delta_2 \phi_2 &= 0 \\ \Delta_2 (1 + u_{h2}L_2) \phi_2 + L_1 \Delta_1 \phi_1 &= 0 \\ \Delta_1 L_1 \phi_1 + \Delta_2 L_2 \phi_2 &= 0 \end{aligned} \quad (B6)$$

Combining, e.g., the first two and the last two equations and each time setting the determinant to be zero and combining with the third equation in (B6), we immediately obtain

$$\begin{aligned} L_1 &= \log \frac{2\Lambda}{\Delta_1} = \frac{1}{u_{hh} - u_{h1}}, \\ L_2 &= \log \frac{2\Lambda}{\Delta_2} = \frac{1}{u_{hh} - u_{h2}}, \end{aligned} \quad (B7)$$

The real parts of the same set of Eqs.(B2) can be evaluated at $\phi_1 = \phi_2 = 0$. The first two equations of the set (B2) with real $\Delta_{hi} = \Delta_i$ are identical for $L_{1,2}$

(and $\Delta_{1,2}$) given by (B7) and using them we can express $\Delta_e L_e = \Delta_e \log \frac{2\Lambda}{|\Delta_e|}$ in terms of various couplings u . Solving for Δ_e and substituting the result into the last equation in (B2) we obtain the expression for $u_{he} = u_{he}^{max}$ for the upper boundary of the TRSB state. The result for u_{he}^{max} for $u_{h2} = u_e = 0$ and $u_{h1} \ll u_{hh}$ is presented in the main text. The result for the lower boundary of the TRSB state, u_{he}^{min} is obtained in a similar manner, by expanding near $\phi_{1,2} = \pi$.

3. TRSB state for angle-dependent interaction

Our primary interest is to study how the TRSB state is modified if outside this state the gaps on the two Γ -centered hole pockets have angular dependence and even accidental nodes, if this dependence is strong enough.

To focus on this physics and avoid lengthy formulas, we ignore potential anisotropy of intra-pocket interactions u_{hi} and u_e and of electron-hole interaction u_{he} , and only include the anisotropy of the interaction u_{hh} between the two Γ -centered hole pockets. By symmetry¹¹, angle-dependence of u_{hh} comes in the form

$$u_{hh}(k, p) = u_{hh} (1 + 2\alpha \cos 4\theta_k + 2\alpha \cos 4\theta_p) + \dots \quad (B8)$$

where dots stand for $\cos 8\theta$, etc terms which we neglect. The most general solution for the hole gaps for this form of the interaction is

$$\begin{aligned} \Delta_{h1} &= \Delta_1 (e^{i\phi_{1a}} + r_1 e^{i\phi_{1b}} \cos 4\theta) \\ \Delta_{h2} &= \Delta_2 (e^{i\phi_{2a}} + r_2 e^{i\phi_{2b}} \cos 4\theta) \\ \Delta_e &= \Delta_3 \end{aligned} \quad (B9)$$

where without loss of generality we can set Δ_i and r_i to be positive. As before, we select Δ_e to be real by adjusting the overall phase.

To obtain the gaps in the TRSB state for arbitrary interactions u , one has to solve the set of nine coupled equations, which can only be done numerically. One can, however, still find an analytical solution for the case $u_{h1} = u_{h2}$. In this situation, two hole pockets are equivalent, and one can easily show that $\Delta_{h1} = \Delta_{h2}^*$. We verified that the set of non-linear gap equations is satisfied if we use the following ansatz

$$\begin{aligned} \Delta_{h1} &= \Delta_{h2}^* = \Delta e^{i\phi/2} (1 + (r_a e^{-i\phi} + r_b) \cos 4\theta) \\ \Delta_e &= -\gamma \Delta \end{aligned} \quad (B10)$$

This ansatz contain five unknowns ($\Delta, \gamma, r_a, r_b, \phi$). Substituting these forms into the set of non-linear gap equa-

tions (Eq. (B2) with u_{hh} given by (B8), we obtain

$$\begin{aligned}
r_a &= -2\alpha u_{hh} \int L_\theta (1 + r_b \cos 4\theta) \\
r_b &= -2\alpha u_{hh} r_a \int L_\theta \cos 4\theta \\
\cos \frac{\phi}{2} &= - \int (u_{hh} A_\theta + u_{h1}) L_\theta (1 + r_b \cos 4\theta) \cos \frac{\phi}{2} \\
&\quad - r_a \int (u_{hh} A_\theta + u_{h1}) L_\theta \cos 4\theta \cos \frac{\phi}{2} \\
&\quad + 2u_{he} L_e \gamma \\
1 &= \int (u_{hh} A_\theta - u_{h1}) L_\theta (1 + r_b \cos 4\theta) \\
&\quad - r_a \int (u_{hh} A_\theta - u_{h1}) L_\theta \cos 4\theta \\
\gamma &= 2u_{he} \int L_\theta \cos \frac{\phi}{2} (1 + (r_a + r_b) \cos 4\theta) \quad (\text{B11})
\end{aligned}$$

where $L_\theta = \ln \frac{2\Lambda}{|\Delta(\theta)|}$ and $A_\theta = 1 + 2\alpha \cos 4\theta$. When $\alpha = 0$, we have $r_a = r_b = 0$, and the other three equations coincide with what we had in the isotropic case.

We analyze this set both analytically and numerically, and found that TRSB state (the one with ϕ different from zero or π) still exists, at $T = 0$, in some range of u_{he} , even if the hole gaps in $+-$ and/or $++$ states have accidental nodes. However, in the TRSB state, the gap amplitude has minima but no nodes, simply because $|\Delta_{h1}| = |\Delta_{h2}| = \Delta^2((1 + (r_a \cos \phi + r_b) \cos 4\theta)^2 + r_a^2 \sin^2 \phi \cos^2 4\theta)$ never hits zero when $\sin \phi$ is non-zero. We discuss this in the main text.

Appendix C: Collective modes

In this Appendix we present some details of the derivation of the dispersion of collective modes.

We consider the minimal model with two equal hole pockets and two inter-pocket interactions u_{he} and u_{hh} . The extension to more general cases is straightforward, but the formulas become more cumbersome.

We include both the pairing interactions (u_{he} and u_{hh}) and 2D long-range Coulomb interaction $V_q = A_2/|q|$, $A_2 = 2\pi e^2$. To obtain the dispersion of collective modes, we add to the system a small frequency and momentum-dependent perturbation (the bare terms)

$$\begin{aligned}
H_{pert} &= \sum_k \left(\delta\Delta_{h1}(0) c_{1\uparrow}^\dagger c_{1\downarrow}^\dagger h.c. \right) + \sum_k [c_1 \leftrightarrow c_2] \\
&\quad + \sum_k [c_1 \leftrightarrow f_1] + \sum_k [c_1 \leftrightarrow f_2] \\
&\quad + \delta\rho(0) \sum (c_1^\dagger c_1 + \dots + f_2^\dagger f_2) \quad (\text{C1})
\end{aligned}$$

where $\delta\Delta_i \equiv \delta\Delta_i(q, \Omega) e^{i(\Omega t - \mathbf{q} \cdot \mathbf{r})}$ and $\Delta\rho \equiv \delta\rho(q, \Omega) e^{i(\Omega t - \mathbf{q} \cdot \mathbf{r})}$, compute fully renormalized $\delta\Delta$ and $\delta\rho$, and obtain collective modes as the poles of the generalized susceptibility. Alternatively, the collective modes can be computed by extending HS approach to finite q and Ω , see Refs. 44,46,49.

The field $\delta\rho(q, \Omega) \equiv \delta\rho$ is real, while $\delta\Delta_i(q, \Omega)$ is generally complex and it is instructive to split it into real and imaginary parts: $\delta\Delta_j(q, \Omega) = \delta_j^R + i\delta_j^I$. If the equilibrium gap Δ_j is real, δ_j^R and δ_j^I describe amplitude (longitudinal) and phase (transverse) fluctuations of the gap. If the equilibrium gap is complex, each of δ_j^R and δ_j^I describes amplitude and phase fluctuations. In particular, if in equilibrium $\Delta_{h1} = \Delta e^{i\phi/2}$, $\Delta_{h2} = \Delta e^{-i\phi/2}$, $\Delta_e = -\gamma\Delta$, the relation between δ_j^R , δ_j^I and the changes of the amplitudes and the phases of the three gaps $[|\Delta_{h1}| \rightarrow \Delta + m_{h1}, \phi/2 \rightarrow \phi/2 + \phi_{h1}; \Delta_{h2} \rightarrow \Delta + m_{h2}, -\phi/2 \rightarrow -\phi/2 + \phi_{h2}; |\Delta_e| \rightarrow -\gamma\Delta + m_e, 0 \rightarrow \phi_e]$ is

$$\begin{pmatrix} \delta_{h1}^R \\ \delta_{h2}^R \\ \delta_e^R \\ \delta_{h1}^I \\ \delta_{h2}^I \\ \delta_e^I \end{pmatrix} = \begin{pmatrix} \cos \frac{\phi}{2} & 0 & 0 & -\sin \frac{\phi}{2} & 0 & 0 \\ 0 & \cos \frac{\phi}{2} & 0 & 0 & \sin \frac{\phi}{2} & 0 \\ 0 & 0 & -1 & 0 & 0 & 0 \\ \sin \frac{\phi}{2} & 0 & 0 & \cos \frac{\phi}{2} & 0 & 0 \\ 0 & -\sin \frac{\phi}{2} & 0 & 0 & \cos \frac{\phi}{2} & 0 \\ 0 & 0 & 0 & 0 & 0 & -\gamma \end{pmatrix} \begin{pmatrix} m_{h1} \\ m_{h2} \\ m_e \\ \Delta \cdot \phi_{h1} \\ \Delta \cdot \phi_{h2} \\ \Delta \cdot \phi_e \end{pmatrix} \quad (\text{C2})$$

Each of the bare vertices gets renormalized by the pairing interactions and long-range Coulomb interaction. At weak coupling, only ladder-type particle-particle renormalizations and small q particle-hole renormalizations are relevant. Collecting the relevant diagrams (see Fig. 4 in the main text), we obtain the set of coupled equations for fully renormalized vertices $\overline{\delta\Delta}_i = \overline{\delta}_i^R + i\overline{\delta}_i^I$ and

$\overline{\delta\rho} = \overline{\delta}_\rho$ as we said in the main text.

The seven branches of collective excitations are obtained from the condition that $\text{Det} \underline{K}(q, \Omega) = 0$. Two of these branches are fluctuations of the overall phase and of the total density, the others are three longitudinal gap fluctuations and two different fluctuations of the relative phases of the three gaps. Some of these fluctuations de-

couple from the others, but some are coupled.

The components of $\Pi_{ii}^{ab}(q, \Omega)$ can be represented in the Nambu formalism as

$$\Pi_{ii}^{ab}(q, \Omega) = \frac{1}{N_0} T \sum_{\omega} \int \frac{d^2 k}{(2\pi)^2} \text{Tr} [\mathcal{G}_i(k, \omega) \sigma^a \mathcal{G}_i(k+q, \omega + \Omega) \sigma^b] \quad (\text{C3})$$

where ω is the fermionic Matsubara frequency, σ^i are the Pauli matrices, and

$$\mathcal{G}_i(k, \omega) = \begin{pmatrix} G_i(k, \omega) & -F_i(k, \omega) \\ -F_i^\dagger(k, \omega) & \tilde{G}_i(k, \omega) \end{pmatrix} \quad (\text{C4})$$

where

$$\begin{aligned} \tilde{G}_i(k, \omega) &= -\frac{i\omega + \varepsilon_{k,i}}{\omega^2 + E_i^2} \\ G_{\downarrow\downarrow} &= -\frac{i\omega - \varepsilon_{k,i}}{\omega^2 + E_i^2} \\ F_{\downarrow\uparrow} &= -\frac{\Delta_i}{\omega^2 + E_i^2} \\ F_{\uparrow\downarrow}^\dagger &= -\frac{\Delta_i^*}{\omega^2 + E_i^2} \end{aligned} \quad (\text{C5})$$

Evaluating the integrals, we find that 21 components of $\underline{\Pi}$ are non-zero.

To properly describe all collective excitations, one should keep the frequency to be of order Δ , as some of the modes exist only as resonances at $\Omega > 2\Delta$. Our goal, however, is more focused as we are only interested in the 2D plasmon mode and in the modes which soften at the boundaries of TRSB state. These modes are the solutions of $\text{Det}\underline{K}(q, \Omega) = 0$ at small Ω , and to get these modes one can safely expand in both $v_F q / \Delta$ and in Ω / Δ .

Evaluating the integrals and converting from Matsubara to real frequency axis we obtain the expressions for Π_{ii}^{jk} and $\underline{K}(q, \Omega)$ at small Ω and \vec{q} , which we presented in Eqs. (6) and (10) in the main text.

Solving for $\text{Det}\underline{K}(q, \Omega) = 0$, we obtain seven branches of collective excitations, which we discuss in the main text. One can show quite generally that fluctuations of the overall phase and of the total density are coupled to each other but decoupled from other five branches of collective excitations. One of coupled oscillation of the overall phase and the total density is a plasmon mode (see the main text). Among the other five modes, longitudinal and transverse fluctuations decouple in $++$ and $+-$ phases, but couple in the TRSB state. This coupling leads to a peculiar structure of low-energy collective excitations near the boundaries of the TRSB state. We present the results in the main text.

1. Plasmon mode in a 3D superconductor

For completeness, we also present the diagrammatic derivation of the dispersion of a plasmon mode (a coupled

oscillation of a phase of a superconductor order parameter and an electron density) in a 3D superconductor. In 3D, plasmon frequency tends to a finite value at $q \rightarrow 0$, and the approximation $\Omega \ll \Delta$, which we used in the previous subsection, is not applicable, at least in the clean limit.

In the dirty limit, the plasmon frequency is small (it can be much smaller than Δ). A general gradient expansion analysis in this case shows⁴³ that the plasma frequency scales with the density of superconducting electrons (the “superfluid density”). In a clean limit, superfluid density coincides with the full density, and it is reasonable to expect that the plasma frequency remains the same as in the normal state.

That the plasma frequency is not renormalized in the clean limit and at $T = 0$ has been argued by Anderson back in 1958 on general grounds (Ref.⁴⁷) and has been shown explicitly by Ohashi and Takada using an RPA formalism, extended to a superconducting state⁴⁸. We reproduce this result in a direct diagrammatic approach, similar to the one we used in the main text for the 2D case. For brevity we consider the case of a single-band s-wave superconductor. The extension to multi-band systems is straightforward.

We follow the same strategy as in the main text – introduce bare particle-particle and particle-hole vertices, which correspond to small variations of a superconducting gap and a total density ($\delta\Delta = \delta^R + i\delta^I$ and $\delta\rho$, respectively), and express the full vertices in terms of the bare ones, using dimensionless $u < 0$ for the pairing interaction and $V_q = A_3/q^2$ for Coulomb interaction in 3D, with $A_3 = 4\pi e^2$. The diagrams for the vertices are shown in Fig. 9

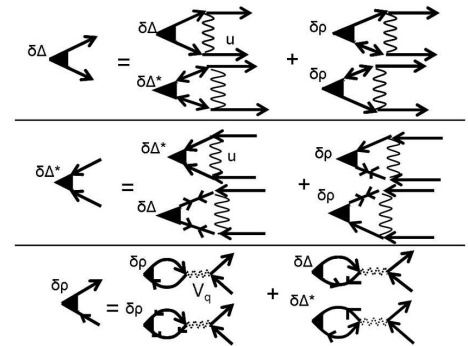


FIG. 9: Diagrammatic representation of the coupled equations for fluctuations of the total density $\delta\rho$ and the SC order parameter $\delta\Delta$ (and $\delta\Delta^*$) for the one band case. The solid and dotted wavy lines represent the pairing interaction $u < 0$ and unscreened Coulomb interaction V_q . The lines with single and double arrows represent the normal (G) and anomalous (F) Green functions. The coupling is due to GF terms which are non-zero when $\vec{q}, \Omega \neq 0$

Like in the previous section, we introduce the vector δ with the components $\delta^R, -\delta^I$, and $\delta\rho$, and write the full

vertex $\bar{\delta}$ in the same was as in (8), but now with

$$\underline{K}(q, \Omega) = \begin{pmatrix} -\frac{2}{u} + \Pi^{11} & 0 & 0 \\ 0 & -\frac{2}{u} + \Pi^{22} & -\Pi^{23} \\ 0 & -\Pi^{32} & -\frac{1}{N_0 V_q} + \Pi^{33} \end{pmatrix} \quad (\text{C6})$$

The zeros indicate that the magnitude fluctuations δ^R do not couple to the phase and density fluctuations (δ^I and $\delta\rho$ terms). The last two fluctuations, however, couple to each other. The dispersion of the collective modes are again obtained from the condition $\text{Det}\underline{K}(q, \Omega) = 0$. The mode which corresponds to coupled phase-density oscillations is obtained from

$$\left(\frac{2}{u} - \Pi^{22}\right) \left(\frac{1}{N_0 V_q} - \Pi^{33}\right) = \Pi^{23} \Pi^{32} \quad (\text{C7})$$

Expanding only in \vec{q} , we get

$$\begin{aligned} \Pi^{23} &= \frac{i\Omega}{2\Delta} \left[\mathcal{I}_\Omega + \left(\frac{Q}{2\Delta}\right)^2 \mathcal{I}_\Omega^{23} \right] \\ \Pi^{32} &= -\Pi^{23} \\ \Pi^{22} &= \frac{2}{u} - \left(\frac{\Omega}{2\Delta}\right)^2 \mathcal{I}_\Omega + \left(\frac{Q}{2\Delta}\right)^2 \mathcal{I}_\Omega^{22} \\ \Pi^{33} &= -\mathcal{I}_\Omega - \left(\frac{Q}{2\Delta}\right)^2 [\mathcal{I}_\Omega^{23} + \mathcal{I}_\Omega^{33}] \end{aligned} \quad (\text{C8})$$

where $E = \sqrt{\epsilon^2 + \Delta^2}$, Λ is the upper cutoff, and $Q^2 = \langle (\vec{v}_F \cdot \vec{q})^2 \rangle = \frac{v_F^2 q^2}{3}$ in 3D (and $\frac{v_F^2 q^2}{2}$ in 2D). In Π^{22} we have used the BCS gap equation that tells us

$$-\frac{2}{u} = \int_\Lambda^\Lambda \frac{d\epsilon}{E} \quad (\text{C9})$$

Also,

$$\begin{aligned} \mathcal{I}_\Omega &= \int \frac{\Delta^2}{E (E^2 - \frac{\Omega^2}{4})} \\ \mathcal{I}_\Omega^{22} &= \int \frac{\Delta^4 (3E^2 - \frac{\Omega^2}{4})}{2E^3 (E^2 - \frac{\Omega^2}{4})^2} \\ \mathcal{I}_\Omega^{23} &= \int \frac{\Delta^4 (E^2 (2E^2 - 5\Delta^2) + (2E^2 - 3\Delta^2) (\frac{\Omega}{2})^2)}{2E^5 (E^2 - \frac{\Omega^2}{4})^2} \\ \mathcal{I}_\Omega^{33} &= \int \frac{\Delta^4}{E^3 (E^2 - \frac{\Omega^2}{4})} \end{aligned} \quad (\text{C10})$$

Eq. C7 now becomes, to the leading order in q :

$$\Omega^2 = N_0 V_q Q^2 \left[\mathcal{I}_\Omega^{22} - \left(\frac{\Omega}{2\Delta}\right)^2 (\mathcal{I}_\Omega^{33} - \mathcal{I}_\Omega^{23}) \right] + O(Q^2) \quad (\text{C11})$$

Using

$$\begin{aligned} \mathcal{I}_\Omega^{22} &= 2 + \left(\frac{\Omega}{2\Delta}\right)^2 \int \frac{\Delta^4 (5E^2 - 2(\frac{\Omega}{2})^2)}{2E^5 (E^2 - \frac{\Omega^2}{4})^2} \\ \mathcal{I}_\Omega^{33} - \mathcal{I}_\Omega^{23} &= \int \frac{\Delta^4 (5E^2 - 2(\frac{\Omega}{2})^2)}{2E^5 (E^2 - \frac{\Omega^2}{4})^2} \end{aligned} \quad (\text{C12})$$

we immediately find that

$$\mathcal{I}_\Omega^{22} - \left(\frac{\Omega}{2\Delta}\right)^2 (\mathcal{I}_\Omega^{33} - \mathcal{I}_\Omega^{23}) = 2 \quad (\text{C13})$$

and hence

$$\Omega^2 = 2N_0 V_q Q^2 \quad (\text{C14})$$

which is the same result as in the normal state. Substituting the expressions for $V_q = 4\pi e^2/q^2$, $Q^2 = v_F^2 q^2/3$, $N_0 = mp_F/(2\pi^2)$, and using the relation between p_F and the density of fermions $p_F^3/(3\pi^2) = n$, we obtain

$$\Omega^2 = \frac{4\pi n e^2}{m} = \Omega_{pl}^2 \quad (\text{C15})$$

which is the same plasma frequency as in the normal state. This result is well-known starting from the Anderson work⁴⁷. Like we said, our goal was just to demonstrate how this result can be re-derived in a direct diagrammatic approach.

At a finite $T \leq T_c$ and/or in the presence of impurity scattering, coupled density and phase fluctuations are more complex, and near T_c there exists a weakly damped, near-gapless Carlson-Goldman mode⁵⁰. The evolution of plasma oscillations with increasing T and/or impurity scattering are not fully understood as only the cases $\Omega = \Omega_{pl}$ and $\Omega \ll \Delta \ll \Omega_{pl}$ have been analyzed in detail (see, e.g., Ref. 44). The diagrammatic approach which we present here offers the way to obtain the results for all T and also with and without impurity scattering.

¹ A.P. Mackenzie, Y. Maeno, Rev. Mod. Phys. **75**, 657712 (2003).

² R.B. Laughlin, Phys. Rev. Lett. **80**, 5188(1998).

³ R. Nandkishore, L.S. Levitov, and A.V. Chubukov, Nat.

Phys. **8**, 158 (2012).

⁴ W.-C. Lee, S.-C. Zhang, and C. Wu, Phys. Rev. Lett. **102**, 217002 (2009).

⁵ K. Suzuki, H. Usui, and K. Kuroki, Phys. Rev. B **84**,

- 144514 (2011).
- ⁶ S. Graser, T.A. Maier, P.J. Hirschfeld, D.J. Scalapino, New J. Phys. **11**, 025016 (2009).
 - ⁷ F. Wang, H Zhai, Y Ran, A. Vishwanath, and D-H Lee, Phys. Rev. Lett. **102**, 047005 (2009).
 - ⁸ R. Thomale, C. Platt, W. Hanke, and B. Andrei Bernevig, Phys. Rev. Lett. **106**, 187003 (2011). See also C. Platt, C. Honerkamp, and W. Hanke, New J. Phys. **11**, 055058 (2009).
 - ⁹ R. Thomale, C. Platt, J. Hu, C. Honerkamp, and B. A. Bernevig, Phys. Rev. B **80**, 180505(R) (2009).
 - ¹⁰ R. Thomale, C Platt, W. Hanke, J. Hu, and B. Andrei Bernevig, Phys. Rev. Lett. **107**, 117001 (2011).
 - ¹¹ S. Maiti, M. M. Korshunov, T. A. Maier, P. J. Hirschfeld, and A. V. Chubukov, Phys. Rev. B **84**, 224505 (2011); Phys. Rev. Lett. **107**, 147002 (2011).
 - ¹² C. Platt, R. Thomale, C. Honerkamp, S.-C Zhang, W. Hanke, Phys. Rev. B **85**, 180502 (2012).
 - ¹³ M. Khodas, A. V. Chubukov, Phys. Rev. Lett. **108**, 247003 (2012).
 - ¹⁴ R. M. Fernandes and A. J. Millis, arXiv:1208.3412 (2012).
 - ¹⁵ V. Stanev and Z. Tesanovic, Phys. Rev. B **81**, 134522 (2010).
 - ¹⁶ D.F. Agtenberg, V. Barzykin, and L.P. Gorkov, Phys. Rev. B **60**, 14868 (1999).
 - ¹⁷ T.K. Ng and N. Nagaosa, Europhys. Lett. **87**, 17003 (2009).
 - ¹⁸ Y. Tanaka and T. Yanagisawa, Solid. State. Comm. **150**, 1980 (2010); T. Yanagisawa, Y. Tanaka, I. Hase, and K. Yamaji, J. Phys. Soc. Jpn. **81** 024712 (2012).
 - ¹⁹ X. Hu and Z. Wang, Phys. Rev. B **85**, 064516 (2011).
 - ²⁰ S.-Z. Lin and X. Hu, Phys. Rev. Lett. **108**, 177005 (2012).
 - ²¹ J. Carlström, J. Garaud, and E. Babaev, Phys. Rev. B **84**, 134518 (2011).
 - ²² G. Livanas, A. Aperis, P. Kotetes, G. Varelogiannis, arXiv:1208.2881 (2012).
 - ²³ V. Stanev, Phys. Rev. B **85**, 174520 (2012).
 - ²⁴ I. Bobkova and A. Bobkov, Phys. Rev. B **84**, 134527 (2011).
 - ²⁵ H. Ding et al., Europhys. Lett. **83**, 47001 (2008).
 - ²⁶ K. Nakayama et al., Phys. Rev. B **83**, 020501 (2011).
 - ²⁷ A.D. Christianson, E.A. Goremychkin, R. Osborn, S. Rosenkranz, M.D. Lumsden, C.D. Malliakas, L.S. Todorov, H. Claus, D.Y. Chung, M.G. Kanatzidis, R.I. Bewley, and T. Guidi, Nature **456**, 930 (2008).
 - ²⁸ R. Khasanov et al., Phys. Rev. Lett. **102**, 187005 (2009).
 - ²⁹ X. G. Luo, M. A. Tanatar, J.-Ph. Reid, H. Shakeripour, N. Doiron-Leyraud, N. Ni, S. L. Budko, P. C. Canfield, Huiqian Luo, Zhaosheng Wang, Hai-Hu Wen, R. Prozorov, and Louis Taillefer Phys. Rev. B **80**, 140503 (2009).
 - ³⁰ J.-Ph. Reid, A. Juneau-Fecteau, R. T. Gordon, S. Rene de Cotret, N. Doiron-Leyraud, X. G. Luo, H. Shakeripour, J. Chang, M. A. Tanatar, H. Kim, R. Prozorov, T. Saito, H. Fukazawa, Y. Kohori, K. Kihou, C. H. Lee, A. Iyo, H. Eisaki, B. Shen, H.-H. Wen, and L. Taillefer, Supercond. Sci. Technol. **25**, 084013 (2012).
 - ³¹ I. I. Mazin, D. J. Singh, M. D. Johannes, and M. H. Du, Phys. Rev. Lett. **101**, 057003 (2008); K. Kuroki, S. Onari, R. Arita, H. Usui, Y. Tanaka, H. Kontani, and H. Aoki, Phys. Rev. Lett. **101**, 087004 (2008); A. V. Chubukov, D. V. Efremov and I Eremin, Phys. Rev. B **78**, 134512 (2008); V. Cvetkovic and Z. Tesanovic, Phys. Rev. B **80**, 024512 (2009); J. Zhang, R. Sknepnek, R. M. Fernandes, and J. Schmalian, Phys. Rev. B **79**, 220502(R) (2009); I.I. Mazin and J. Schmalian, Physica C., **469**, 614 (2009); A. F. Kemper, T. A. Maier, S. Graser, H-P. Cheng, P. J. Hirschfeld and D. J. Scalapino, New J. Phys. **12**, 073030 (2010); P. J. Hirschfeld, M. M. Korshunov, I. I. Mazin Rep. Prog. Phys. **74**, 124508 (2011); A. V. Chubukov, Annu. Rev. Cond. Matt. Phys., **3**, 57 (2012).
 - ³² K. Okazaki and S. Shin, private communication.
 - ³³ T. Sato, K. Nakayama, Y. Sekiba, P. Richard, Y.-M. Xu, S. Souma, T. Takahashi, G. F. Chen, J. L. Luo, N. L. Wang, H. Ding, Phys. Rev. Lett. **103**, 047002 (2009).
 - ³⁴ K. Okazaki, Y. Ota, Y. Kotani, W. Malaeb, Y. Ishida, T. Shimojima, T. Kiss, S. Watanabe, C.-T. Chen, K. Kihou, C. H. Lee, A. Iyo, H. Eisaki, T. Saito, H. Fukazawa, Y. Kohori, K. Hashimoto, T. Shibauchi, Y. Matsuda, H. Ikeda, H. Miyahara, R. Arita, A. Chainani, S. Shin, Science, **337**, 1314(2012).
 - ³⁵ S. Maiti, M. M. Korshunov, and A. V. Chubukov, Phys. Rev. B **85**, 014511 (2012).
 - ³⁶ J.-Ph. Reid, M. A. Tanatar, A. Juneau-Fecteau, R. T. Gordon, S. Rene de Cotret, N. Doiron-Leyraud, T. Saito, H. Fukazawa, Y. Kohori, K. Kihou, C. H. Lee, A. Iyo, H. Eisaki, R. Prozorov, Louis Taillefer, Phys. Rev. Lett. **109**, 087001 (2012).
 - ³⁷ A. F. Wang, S. Y. Zhou, X. G. Luo, X. C. Hong, Y. J. Yan, J. J. Ying, P. Cheng, G. J. Ye, Z. J. Xiang, S. Y. Li, and X. H. Chen, arXiv 1206.2030.
 - ³⁸ M. Abdel-Hafiez, V. Grinenko, S. Aswartham, I. Morozov, M. Roslova, O. Vakaliuk, S.-L. Drechsler, S. Johnston, D. V. Efremov, J. van den Brink, H. Rosner, M. Kumar, C. Hess, S. Wurmehl, A. U. B. Wolter, B. Buechner, E. L. Green, J. Wosnitza, P. Vogt, A. Reifemberger, C. Enss, and R. Klingeler, arXiv:1301.5257.
 - ³⁹ T. Shibauchi, private communication.
 - ⁴⁰ A. V. Chubukov, Physica C **469**, 640 (2009); S. Maiti, A. V. Chubukov Phys. Rev. B **82**, 214515 (2010).
 - ⁴¹ A. J. Leggett, Prog. of Theor. Phys. **36**, 901 (1966).
 - ⁴² R. Côte, A. Griffin, Phys. Rev. B **48**, 10404(1993);
 - ⁴³ For the discussion on the plasmon mode in a dirty s-wave superconductor see B. Narozhny, A.I. Aleiner and B.L. Altshuler, Phys. Rev. B. **60**, 7213 (1999); A. Kamenev, *Field Theory of Non-Equilibrium systems*, Cambridge University Press, 2011 and references therein.
 - ⁴⁴ S.N. Artemenko and A.F. Volkov, Usp. Fiz. Nauk. **128**, 3 (1979) (Sov. Phys. Usp. **22**, 295 (1979)); I.O. Kulik, O. Entin-Wohlman, and R. Orbach J. Low Temp. Phys. **43** 591 (1981); J.E. Mooij and G. Schon, Phys. Rev. Lett. **55**, 114 (1985); S.G. Sharapov, V.P. Gusynin and H. Beck, Euro. Phys. Jour. B **30** 45, (2002); S.G. Sharapov and H. Beck, Phys. Rev. B **65**, 134516 (2002).
 - ⁴⁵ L. Benfatto, private communication.
 - ⁴⁶ L. Benfatto, A. Toschi, and S. Caprara, Phys. Rev. B **69**, 184510 (2004).
 - ⁴⁷ P.W. Anderson, Phys. Rev. B **112**, 1900 (1958).
 - ⁴⁸ Y. Ohashi and S. Takada, Journal. of Phys. Soc. Jap., **67**, 551 (1998)
 - ⁴⁹ L. Fanfarillo, L. Benfatto, S. Caprara, C. Castellani, and M. Grilli, Phys. Rev. B **79**, 172508 (2009).
 - ⁵⁰ R.V. Carlson and A.M. Goldman, Phys. Rev. Lett. **34**, 11 (1975).